

Corundum and Bauxite-based Concretes – Non-destructive Testing of Mechanical Properties and its Correlation with the Sintering Process

A. Terzic', L. Pavlovic'

This manuscript presents a new approach on correlation between sintering process, porosity and an important thermo-mechanical property of refractory concrete – creep. A non-destructive test method was applied on the corundum- and bauxite-based refractory concretes, i.e. ultrasonic pulse velocity and also Image Pro Plus program for image analysis. Progression of sintering process can be monitored by the change of the porosity parameters determined with ultrasonic pulse velocity and image analysis. Investigated concretes are varying in chemical and mineral composition. Apparent porosity of samples thermally treated at 110, 800, 1000, 1300 and 1500 °C was primary investigated with standard laboratory procedure. Sintering parameters were calculated from the creep testing. Loss of strength and material degradation occurred in concrete when it was subjected to increased temperature and compressive load. Mechanical properties indicate and monitor changes within microstructure. Level of surface deterioration after thermal treatment was determined using Image Pro Plus image analysis program. Mechanical strength was determined using ultrasonic pulse velocity testing. Investigations presented in this paper confirm that results of creep deformation testing, image analysis and ultrasonic pulse velocity testing are interconnected and that they are a means to monitor the sintering process within concrete exposed to high temperature. Mentioned interconnection can be useful when type of high temperature concrete is to be chosen for application in a metallurgical furnace or some other plant operating at high temperature.

conomic aspect i.e. cheaper process of manufacturing, the possibility of repairing damaged linings, etc [1].

2 Methodology and technical aspects of investigation

Mechanical strength of refractory concrete determines its performance in different applications and it is measured in terms of applied compressive load which concrete can withstand at various temperatures. When concrete is subjected to increasing compressive load and temperature, microstructure of the material changes: apparent porosity increases, pores become bigger and cracks occur within the structure, all resulting in loss of strength and composite degradation. Crack formation and increasing porosity decrease the density and elastic properties of the material. Therefore, measuring either of these properties can directly monitor the development and change of the microstructure. This can be performed by measuring the velocity of ultrasonic pulses (V_p) travelling through the refractory concrete specimen [2].

Non-destructive testing method is preferred due to its evident advantage over conventional compression testing. The method is simple and rapid, there is no need for the destruction of specimens, thus the specimens can be used afterwards, etc. The application of the ultrasonic pulse velocity (UPV) test in the non-destructive evaluation of concrete quality has been investigated for decades. This non-destructive testing method has proved to be of real importance as a useful tool for inspecting the concrete quality in metallurgical furnaces. The evaluation by non-destructive methods of the actual compressive strength of concrete in existing structural elements is based on the empirical relationships between strength and non-destructive parameters. Furthermore, mechanical strength is a direct function of the concrete's porosity and its level of degradation. Manufacturers of UPV devices usually provide empirical relationships for their own testing

1 Introduction

Refractory concretes are commonly used as constructive elements and linings of metallurgical furnaces and other plants operating at high temperatures (linings for oil refinery plants, thermal insulation in plants and in objects, linings in nuclear power plants, linings in chemical and petrochemical industries, etc.). Benefits from application of concrete instead of common refractory materials are as follows: simplified building of refractory linings, eco-

Anja Terzic', Ljubica Pavlovic'
Institute for Technology of Nuclear and
other Raw Mineral Materials
11000 Belgrade, Serbia

Corresponding author: Anja Terzic'
E-mail: anja.terzic@gmail.com

Keywords: ultrasonic pulse velocity, sintering, porosity, refractory concrete, image analysis, creep

Tab. 1 Mix design parameters for C and B concretes

	C	B
Cement [%]	20	30
Water [%]	(12 – 14 at 100 %)	(12 – 14 at 100 %)
Aggregate [%]	80	40 + 30
w/c	0,5	0,6
Green bulk density [g/cm ³]	2,92	2,54

systems. Such relationships are not suitable for every kind of concrete. Therefore, they need to be calibrated for different mixtures [3, 4]. Commonly used formula is:

$$S = a \cdot \exp(b \cdot V_p) \quad (1)$$

where are:

a and b - empirical parameters determined by the least squares method

S - concrete compressive strength

V_p - ultrasonic pulse velocity of longitudinal waves

Most factors that influence concrete strength also influence pulse velocity, though not necessarily in the same way or to the same extent. The presence of aggregates affects the relationship between pulse velocity and the compressive strength: concrete with the highest aggregate content will probably have the highest pulse velocity [5]. The cement type influences pulse velocity and also the compressive strength of concrete. Higher water content affects the propagation velocity approximately in proportion to the change of the water content in concrete [6].

A review of the literature indicated that ultrasonic waves are used to predict different properties of concrete. For example: residual properties of thermally damaged concrete [7], the initial degree of hydration of concrete [8], etc. This method can also be used to detect internal defects of concrete such as cracks, delamination and/or honeycombs, and porosity for the characterization of microstructural defects [9–13].

UPV technique can be accompanied by other non-destructive monitoring methods such as for example the program for image analysis. The application of an optical microscope connected to a computer with an image analysis program enables an entirely new group of properties to be described: the number of pores situated within surfacial pores, the shape and size of pores or cracks, pore roundness, etc. In this paper, the apparent porosity level was

monitored after each thermal treatment using the Image Pro Plus (IPP) program for image analysis and the results were correlated with the results of the ultrasonic measurement [14]. It should be noted here that the apparent porosity of refractory composites is increasing with temperature until a certain level is achieved. Namely, the sintering process of refractory materials occurs due to the constant elevation of temperature: grouped pores are gaining spherical shape and start to diminish. Sintering process initiates a thickening of the material at elevated temperatures (above 1300 °C for an average high-temperature concrete).

The objective of this work is to use the non-destructive testing method (UPV) and image analysis (IPP) and their advantages to predict the behaviour of concrete submitted to compressive loads and increased temperatures. Thus the main concern is the determination of the apparent porosity levels of concrete during the sintering process using the ultrasonic pulse velocity technique and image analysis.

3 Materials and experimental procedure

3.1 Materials

Two series of refractory concrete samples of different composition (2 x 60 samples), hereafter indicated as C and B, were investigated. The concrete samples contained different volume fractions and different types of refractory aggregates (Tabs. 1 and 2). First type of concrete (sample B) contained bauxite and chamotte as aggregates and it can be classified as commercially available concrete. The other type of concrete (sample C) was pre-

pared with corundum as aggregate and it can be classified as experimental concrete. The aggregates had different grain sizes. Both types of concrete were prepared with high aluminate cement SECAR70 (*Kerneos*).

The chemical compositions of the investigated concretes B and C and the cement used are given in Tab. 3.

3.2 Mechanical compressive strength – destructive testing method

Refractory concretes C and B were investigated for their mechanical compressive strength according to the standard laboratory procedure [Standard: JUS B. D8. 304]. Sixty cubic samples of each series (10 cubes for each temperature: 20, 110, 800, 1000, 1300 and 1500 °C) with identical dimensions (10 cm x 10 cm x 10 cm) were investigated. After 7 d of curing in a climate chamber (at 20 °C), the specimens were de-moulded and stored for another 21 d under the same conditions as in the climate chamber. After 28 d, the specimens were dried at 110 °C

Tab. 2 Aggregate granulation for C and B concrete

Aggregate	C	B
Corundum aggregate size [mm]		
-5 +3		
-3 +2	28	
-2 +1	22	
-1 +0,5	28	
-0,5 +0	12	
	10	
Bauxite aggregate size [mm]		
-6 +4		15
-4 +1		55
-1 +0		30
Chamotte aggregate size [µm]		
-74		7,56
-74 +44		18,23
-44 +33		17,59
-33 -23		7,93
-23 +15		17,53
-15 -0		31,16

Tab. 3 Chemical composition of cement and concretes C and B

Oxide [%]	Al ₂ O ₃	SiO ₂	CaO	MgO	Fe ₂ O ₃	Na ₂ O	K ₂ O	TiO ₂
Cement	68,85	0,107	29,73	0,137	0,058	0,285	0,0078	< 0,01
B	62,88	21,17	8,26	0,35	1,57	0,059	0,56	2,03
C	93,62	0,07	8,26	0,03	0,066	0,21	–	0,007

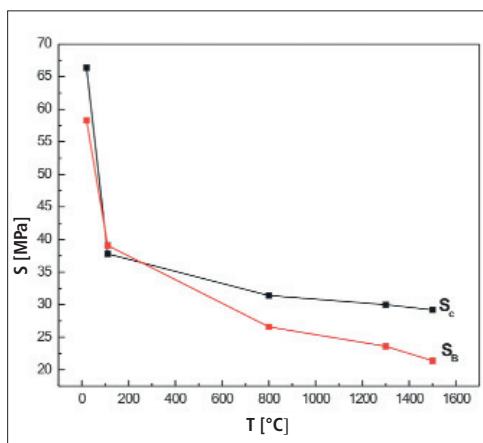


Fig. 1 Mechanical compressive strength degradation S_C [MPa] of concrete C and S_B [MPa] of concrete B

for another 24 h, then transferred into an electric furnace and fired at 800, 1000, 1300 and 1500 °C in groups of 10 specimens and with 4 h soaking at each temperature for each group of specimens. Following this, each group of concrete specimens was tested for mechanical compressive strength using a conventional laboratory-type hydraulic pressure device. The same specimens had previously been subjected to UPV testing and IPP analysis.

3.3 Apparent porosity and image analysis

The apparent porosity of the refractory concrete specimens was determined with an optical microscope (Olympus, CX31-P) in conjunction with a computer program for image analysis. The original microscope images were transmitted to the image processor by a colour camera. The Image Pro Plus (IPP) program (Materials Pro Analyzer, Version 3.1, Media Cybernetics, Silver Spring, MD, USA) was used in the experiment.

The specimens were covered with a thin chalk-powder film before the surface damage was investigated. Areas without damage are coloured by the chalk powder while the damaged areas keep the basic colour of the refractory materials. The film provided better contrast and differentiation of damaged and non-damaged surfaces.

Digital photographs of the specimen surfaces were taken after each thermal treatment and after compressive strength testing (the same specimens from compressive strength testing were used). Different (damaged and non-damaged) surfaces of the specimens were marked with different colours using IPP tools. Thus

higher resolution and sharper differences between damaged and non-damaged surfaces on the specimens could be obtained. When the appropriate colour is selected, it is possible to quantitatively measure the ratio and level of damaged and non-damaged areas by means of image analysis using a statistical approach. The images processed in the analyzer were converted into binary form as white features in front of the black background. The binary images were filtered to reduce as much as possible the other features captured together with the targeted crack images. Enhanced images were ready for quantitative analysis. The program has a procedure for the systematic collection of image analysis data by dividing the total observation area into squares. Following a similar procedure, a transparent grid was attached to each plane section before the analysis. IPP basically works by comparing colours of different objects and calculating squares in marked areas.

At least 10 photographs per specimen were analyzed in order to obtain a reliable characterization of the microstructure. The ratio between specimen surface area and damaged surface area was calculated for each concrete specimen and thus the apparent surface porosity was determined.

3.3 Non-destructive testing method – ultrasonic pulse velocity

A commercial ultrasonic transmission-type testing instrument (PUNDIT plus PC1006, CNS Farnell Ltd, Hertfordshire, England) was used in the experiment. The instrument is equipped with a pulse generator and timing circuit coupled to two transducers (220 kHz) that were manually positioned at opposite ends of each specimen. Each transducer had a 2 mm thick rubber tip to help overcome measurement problems due to the roughness of the refractory surface. Pulses of longitudinal elastic stress waves are generated by an electro-acoustic transducer, which is held in direct contact with the surface of the specimen. The pulses travel through the material and at the end of the path they are received and converted into electric energy by a second transducer. Most standards describe three possible arrangements for the transducers:

- the transducers are located diagonally to each other, that is, the transducers are across corners (diagonal transmission)

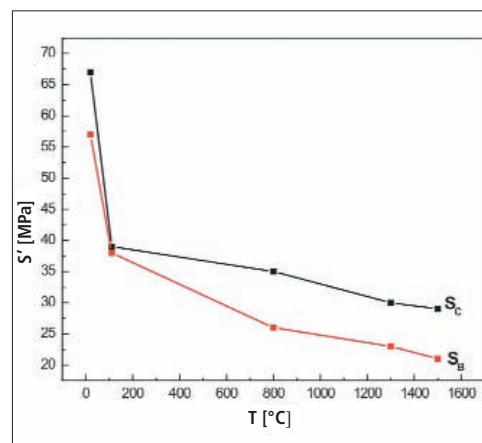


Fig. 2 Mechanical compressive strength degradation S'_C [MPa] of concrete C and S'_B [MPa] of concrete B (calculated using UPV)

- the transducers are located directly opposite to each other (direct transmission)
- the transducers are attached to the same surface and separated by a known distance (indirect transmission).

Direct transmission is the most sensitive and it was applied in this experiment. The transducers were placed on two parallel surfaces of the specimens. Vaseline grease was used as the coupling medium. Sixty concrete specimens of each series with identical dimensions (10 cm x 10 cm x 10 cm) were investigated. For each specimen, measurements of ultrasonic pulse velocity through the length and thickness on direct transmission disposition were performed. Each test was run at least five times to correctly validate the ultrasonic velocity. The same specimens as in compressive strength investigation were used in the UPV analysis. Testing was performed according to valid standards [Standard: JUS.D.B8.121].

The ultrasonic pulse velocity (V_p) is calculated from the distance between the two transducers and the transit time of the pulse measured by an oscilloscope as:

$$V_p = l \cdot t \text{ [m/s]} \quad (2)$$

where:

- l – the stress wave path length [m]
- t – the transit time [s]

Mechanical compressive strength can be approximately calculated from ultrasonic velocity values obtained as is shown by equation (3):

$$S = S_0 (V_p / V_{p0})^n \text{ [MPa]} \quad (3)$$

where:

S_0 – compressive strength before exposure of the material to thermal treatment [MPa]
 v_p – longitudinal ultrasonic velocity after testing [m/s]
 v_{p0} – longitudinal ultrasonic velocity before testing [m/s]
 n – the material constant ($n = 0,488$) accepted from literature and taken as average for both materials [15, 16].

3.4 Creep testing and sintering process

Creep testing was performed on twenty cylindrical concrete specimens, with 10 each of types C and B ($h/d = 50/50$ mm). A hole (diameter 5 mm) was drilled in the centre of each concrete specimen in order to position the thermocouple. The concrete specimens were dried at 110 °C for 24 h and afterwards pre-fired at 800 °C for 4 h. The pre-fired specimens were heated at rate of 5 °C/min from room temperature to testing temperature (1000, 1300 or 1500 °C) in a compression creep apparatus (*Netzsch*, Germany) and then submitted to a static constant compressive load (0,2 MPa) at temperatures of 1000, 1300 and 1500 °C. Each test lasted 30 h. During this period, secondary state of creep was reached. The investigations were performed according to valid standards [Standard: JUS.D.B8.308].

If x is a property of the high-temperature concrete which varies during the sintering process and t is the duration of the sintering process then sintering process can be described with power-law creep:

$$x = k \cdot t^n \quad (4)$$

where:

k – time constant,

n – constant which describes mechanism of sintering.

If the variable x is the dimensional change, then:

$$\Delta l / l_0 = k \cdot t^n \quad (5)$$

where:

$\Delta l = (l_0 - l)$ – linear dimensional change of a concrete specimen [mm]

l_0 – initial linear dimension of a concrete specimen [mm]

The activation energy of the sintering process can be calculated using the equation:

$$E = (R \cdot T_1 \cdot T_2 / (T_1 - T_2)) \cdot \ln (v_1 / v_2) \quad (6)$$

where:

E – activation energy [kJ/mol]

R – gas constant [J/mol · °C]

T – temperature [°C]

v – rate of sintering process ($v = \Delta l / \Delta t$) [mm/min]

Δl – linear dimensional change of a specimen, and

Δt – duration of linear dimensional change process

A combination of equations (5) and (6) gives:

$$\Delta l / l_0 = c \cdot T_2 \cdot \exp (-E / R \cdot T) \quad (7)$$

where c is a constant of material.

Sintering is the process of densification (thickening) of the material, which takes place at elevated temperature (generally above 800 °C, but the threshold of sintering depends on the properties of the material). Structural changes in the material are caused by elevated temperature and compressive loads: pores become spherical and they start to diminish and towards the end of process the smallest pores vanish. Final result is an increase in material density and a decrease in porosity, which improves the thermo-mechanical properties of the material. In case of the high-temperature concrete, sintering can be investigated during the secondary state creep phase (when creep deformation is almost constant and does not depend on time). This corresponds to isothermal sintering under pressure. Thus, the sintering equations can be applied to the results obtained.

4 Results and discussion

The average values of the mechanical compressive strength S [MPa] for specimens C and B, as obtained by destructive method described in section 3.2, are presented in Fig. 1. Fig. 2 presents the average values of mechanical compressive strength S' [MPa] calculated from ultrasonic pulse velocity V_p [m/s] obtained using the non-destructive testing method (described in 3.2). The mechanical strength values obtained by both methods are approximately the same, as can be seen in Figs. 1 and 2. This justifies the application of UPV in the compressive strength determination.

Fig. 1 describes mechanical compressive strength degradation caused by increasing temperature. As it can be seen, specimen C shows higher initial mechanical compressive strength (at 20 °C) and also higher final strength (at 1500 °C) than concrete B. The dif-

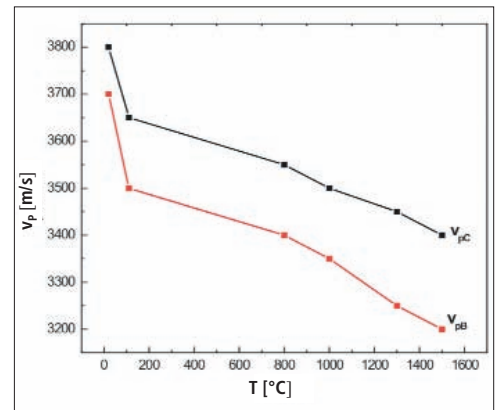


Fig. 3 Ultrasonic pulse velocity v_{pC} [m/s] of concrete C and v_{pB} [m/s] of concrete B

ferences in strength values (at 20 and 1500 °C) are 12,2 and 26,7 %, respectively. The existence of compressive strength degradation points to a microstructure change occurring within the composites. It is evident that specimen C shows slower rate of strength degradation than specimen B during thermal treatment (from 110 °C to 1500 °C). Thus, there are differences in the development of the microstructure of these two concrete samples, probably due to the better choice of grain-size distribution in the case of sample C. Real closure of pores and improvement of mechanical properties cannot be expected below 1500 °C due to the high refractoriness of both materials.

Fig. 3 shows dependence between the calculated average values of ultrasonic pulse velocity V_p [m/s] measured through various concrete specimens (C and B) and increasing temperatures T [°C]. V_p was calculated using formula (2) for each specimen and the average value was determined afterwards.

When Figs. 1 and 2 were compared with Fig. 3, conclusions could be drawn about the correlation between the compressive strength of the composites and the ultrasonic pulse velocity: the lower the compressive strength value, the slower the ultrasonic pulse velocity. The reason for the decrease in mechanical compressive strength and ultrasonic pulse velocity is the degradation, which occurs in concrete microstructures, i.e. the increasing level of porosity. Thus, the UPV method can be used instead of the classical laboratory methods (for example mercury porosimeter) as a means of monitoring of changes in porosity, if it is not necessary to know the precise level of apparent porosity for an experiment.

The changes in average apparent porosity P [%] as a function of increasing temperature

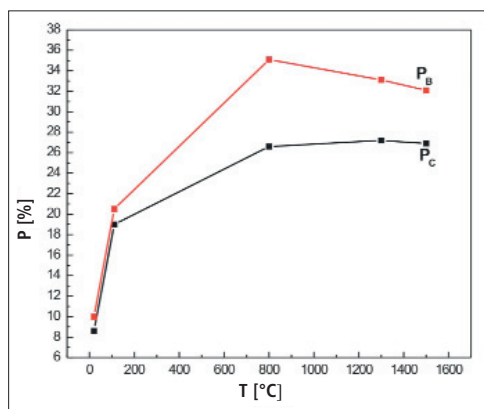


Fig. 4 Change of apparent porosity P_C [%] of concrete C and P_B [%] of concrete B (obtained with IPP)

for samples C and B obtained by the IPP method (described in chapter 3.3) are given in Fig. 4.

The porosity of concrete C is lower than that of concrete B at all investigated temperatures (from 20 to 1500 °C), probably due to the better grain-size distribution and better mix design parameters of concrete C. The difference in the final apparent porosity values is significant: the apparent porosity of sample B is 16,2 % higher than the corresponding value of sample C. This justifies and explains the assumption regarding the cause of the higher degradation of compressive strength of the B samples, i.e. higher porosity means lower mechanical strength.

A peak in both curves (in the case of samples C and B) at 800 °C can be noted in Fig. 4. The peak corresponds to the beginning of the sintering process. Namely, when concrete undergoes thermal treatment, the sintering process occurs at a specific temperature. That usually happens in the temperature interval from 800 to 900 °C. The consequence of sintering would be: a decrease in porosity, a thickening of the material, a compressive strength increase as a result of lower porosity and higher density, etc. However, in this case, both composites (C and

B) have high refractoriness, thus a significant reduction in porosity and an increment in compressive strength are delayed until the thermal interval above 1500 °C. IPP also provides other parameters such as maximum, minimum and average pore diameters (D_{max} , D_{min} , D_{av}), pore roundness (R) and number (N) of pores situated within superficial pores. The results are presented in Tab. 4. According to IPP analysis, the average pore diameter increases from 0,0067 mm (for C concrete) and 0,003 mm (for B concrete) to 0,0089 mm (C) and 0,004 mm (B) at 1300 °C temperature. Afterwards, pore shrinkage occurs as a consequence of the sintering process. Sample B has a smaller average pore diameter although its apparent porosity is higher at all testing temperatures. This is a consequence of the choice of aggregate granulation, i.e. in case of concrete B very fine chamotte aggregate (often referred to as "chamotte flour") was used as the filler. The ideal pore roundness would be 1,00. The pore roundness of the investigated concretes is 1,07 to 1,17, which means that the pores are almost spherical. N is smaller for sample C, which also indicates that the apparent porosity of concrete C is lower than that of concrete B, i.e. most of pores are surface pores.

The UPV non-destructive testing method was applied to the concrete samples in order to investigate possible structural defects and the presence of pores, and to confirm parameters such as mechanical strength. The number of defects and degree of porosity relates directly to the specific test temperature. The sample with the higher ultrasonic puls velocity – in this case concrete sample C – has fewer defects and a lower degree of porosity. Thus, higher porosity in a sample indicates lower ultrasound velocity. The correlation between mechanical strength and ultrasonic velocity is to a certain extent the reverse correlation between porosity and ultrasonic velocity. Regarding the fact that the results for porosity are obtained by IPP

and results for mechanical strength via UPV (compatible with laboratory method) it can be concluded that the use of these two methods confirms the correlation between mechanical strength and porosity and these methods can be used in monitoring and predicting the behaviour of a material.

The results of creep investigation are presented in Fig. 5. It can be seen that the linear dimensional change of sample C at all investigated temperatures is somewhat higher than in the case of B concrete. This was expected because the average pore diameter of concrete C is larger than in the case of concrete B. There is no significant linear change during creep testing at 1000 °C. At 1300 °C the curves dip slightly after 5 h, which might be due to the start of sintering. The decrease at 1500 °C registered after 5 h (for C) and after 10 h (for B) indicates that the sintering process has already begun and porosity is decreasing. Since linear change is the result of pore closure, this means that decrease in porosity will occur sooner in material with lower apparent porosity. This consequently implies that porosity of sample C is lower than porosity of sample B, which confirms the results of IPP and UPV testing.

The results obtained with IPP and UPV methods, i.e. higher porosity in the case of sample B, although the pores in sample C are bigger, can be also seen on the SEM photomicrographs (Figs. 6 and 7) (SEM JEOL JSM-5300). It can also be seen that most of the pores gained a spherical shape at 1500 °C as a result of the sintering process.

5 Conclusions

The aim of this paper was to explain new possibilities of application of a non-destructive testing method – ultrasonic pulse velocity and computer image analysis combined with traditional methods (creep testing and the destructive testing method for compressive mechanical strength) in the description of the sintering process. Besides, an attempt was made to compare the properties of commercially available (bauxite based) and experimental concrete (corundum based) in order to introduce corundum concrete as the better choice for possible applications at high temperatures. Since the UPV method was used to determine ultrasonic velocity and to monitor the compressive strength of refractory composites and Image Pro Plus program to investigate apparent porosity, pore distribution and pore size of concrete samples, the results presented in this

Tab. 4 Results of Image Pro Plus analysis for concrete samples C and B

T [°C]	C					B				
	D_{max} [mm]	D_{min} [mm]	D_{av} [mm]	N	R	D_{max} [mm]	D_{min} [mm]	D_{av} [mm]	N	R
110	0,046	0,0042	0,0067	9	1,08	0,056	0,00129	0,003	51	1,07
800	0,057	0,00448	0,0077	14	1,1	0,073	0,00137	0,0035	74	1,12
1000	0,072	0,0045	0,0084	22	1,13	0,079	0,00138	0,0037	81	1,14
1300	0,089	0,0046	0,0089	26	1,138	0,085	0,00138	0,004	80	1,22
1500	0,084	0,00455	0,0086	24	1,091	0,082	0,00130	0,0038	75	1,17

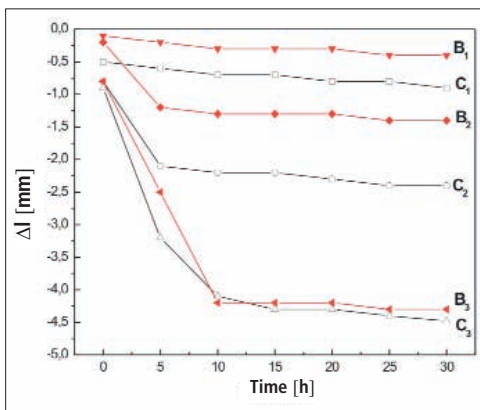


Fig. 5 Creep deformation curves (Δl) obtained during creep tests on B and C sample at three temperatures: B1 and C1 – at 1000 °C, B2 and C2 – at 1300 °C and B3 and C3 – at 1500 °C

paper contribute to the idea of introducing other testing – e.g. non-destructive – testing methods for the determination of mechanical properties, instead of commonly used standard laboratory procedures. It should be noted that non-destructive testing methods, such as UPV, have seldom been used in high-temperature concrete investigations, so UPV can be considered a new method here, although it has a long history of applications in other fields.

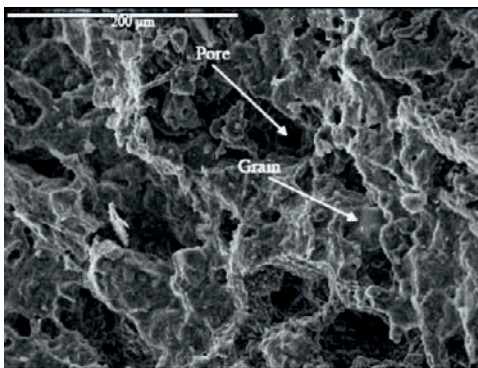


Fig. 6 SEM of B concrete sample heat treated at 1500 °C

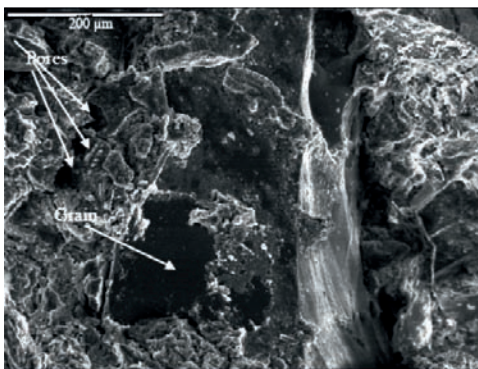


Fig. 7 SEM of C refractory concrete heat treated at 1500 °C

Benefits from using ultrasonic measurements are:

- it is a non-destructive, simple, fast and reliable method
- the same specimens can be used for further tests
- there is a financial benefit in minimizing number of specimens for testing – savings in material and in time
- the results and parameters obtained such as ultrasonic pulse velocity can be correlated with the results obtained by other methods: apparent porosity, mechanical strength, etc.

The UPV can be used to predict high-temperature concrete behaviour and also in monitoring the behaviour of structural concrete elements and refractory linings of metallurgical furnaces. The advantage of this method lies in the fact that there is no need to damage the furnace lining in order to investigate required parameters.

The benefits of using image analysis are also numerous: it provides entirely new and important information about structural damages and surface porosity like, for example, the precise diameters of pores, pore roundness, the number of pores in a section, etc. As surface damage level is measured, the results could be useful for predicting sample behavior during further testing or application in a metallurgical furnace or in thermal insulation.

During UPV and IPP testing it was also concluded that the experimental refractory concrete (in text referred to as C – corundum concrete) possesses better mechanical and thermal characteristics than commercially available bauxite concrete due to its better aggregate properties and granulation and better mix parameter design.

Acknowledgement

This work has been supported by Serbian Ministry of Science (Project 19012 and 16004).

References

[1] Bazant, Z.; Kaplan, M.F.: Concrete at high temperatures, material properties and mathematical models. Concrete Design and Construction Series, Longman Group, London, 1996

[2] Volkov-Husovic, T.; Majstorovic, J.; Cvetkovic, M.: Thermal stability of alumina-based refractory. Am. Ceram. Soc. Bull. 85 (2006) [3] 14–18

[3] Kewalramani, M., Gupta, R.: Concrete compressive strength prediction using ultrasonic pulse velocity through artificial neural networks. Automation in Construction 15 (2006) 374–379

[4] Nehdi, M.; Chabib, H.E.; Naggar, A.: Predicting performance of self-compacting concrete mixtures using artificial neural networks. ACI Mat. J. 98 (2001) [5] 394–401

[5] Crawford, G.I.: Guide to non-destructive testing of concrete. Techn. Rep. No. FHWA-SA-97-105, U.S. Dept. of Transportation, September, 1997

[6] Ohndaira, E.; Masuzawa, N.: Water content and its effect on ultrasound propagation in concrete – the possibility of NDE. Ultrasonics 38 (2000) 546–552

[7] Biolzi, L.; Cattaneo, S.; Rosati, G.: Evaluating residual properties of thermally damaged concrete. Cem. Concr. Comp. 30 (2008) [10] 907–916

[8] Krauß, M.; Hariri, K.: Determination of initial degree of hydration for improvement of early-age properties of concrete using ultrasonic wave propagation. Cement and Concrete Composites 28 (2006) [4] 299–306

[9] Aggelis, D.G.; Shiotani, T.: Repair evaluation of concrete cracks using surface and through-transmission wave measurements. Cem. Concr. Comp. 29 (2007) [9] 700–711

[10] Fu, F.Y.; Wong, Y.L.; Tang, C.A.; Poon, C.S.: Thermal induced stress and associated cracking in cement-based composite at elevated temperatures, Part II: Thermal cracking around multiple inclusions. Cem. Concr. Comp. 26 (2004) [2] 113–126

[11] Malhotra, V.; Carino, N.: CRC Handbook on non-destructive testing of concrete. Boca Raton, FL: CRC Press, 1991

[12] Abo-Qudais, S.A.: Effect of concrete mixing parameters on propagation of ultrasonic waves. Constr. Build. Mat. 19 (2005) 257–263

[13] Boccaccini, D.N.; Canio, M.; Volkov-Husovic, T.: Service life prediction for refractory materials. J. Mat. Sci. 43 (2007) [12] 4079–4090

[14] Volkov-Husovic, T.; Jancic, R.; Mitrakovic, D.: Image analysis used to predict thermal stability of refractories. Am. Ceram. Soc. Bull. 84 (2005) [10] 1–5

[15] Miller, W.: Refractory evaluations with pulse ultrasonic. Presented at the 82nd Annual Meeting of the Am. Ceram. Soc., Chicago, IL/USA, April 28, 1980

[16] Boccaccini, D.N.; Romagnoli, M.; Kamseu, E.; Veronesi, P.; Leonelli, C.; Pellacani, G.C.: Determination of thermal shock resistance in refractory materials by ultrasonic pulse velocity measurements. J. Eur. Ceram. Soc. 27 (2007) [2/3] 1859–1863

[17] Russell, R.O.; Morrow, G.D.: Sonic velocity quality control of steel plant refractories. Am. Ceram. Soc. Bull. 63 (1984) [7] 911–914

[18] Lawlar, J.G.; Ross, R.H.; Rub, E.: Non-destructive ultrasonic testing of fireclay refractories. Am. Ceram. Soc. Bull. 60 (1981) [7] 713–718

[19] Quintela, M.A.; Melo, T.M.F.; Lage, I.J.; Rodrigues, J.A.; Pandolfelli, V.C.: Ceramic shock resistance of carbon-containing refractories. Refractories Manual (2003) 40–44



World

Congress & Exhibition

Exhibition Space NOW AVAILABLE

An "all topic" Technical Programme of Keynote Oral and Poster Presentations

10th - 14th October 2010

Fortezza da Basso Congress Centre, Florence, Italy



www.epma.com/pm2010

